doi:10.1111/j.1558-5646.2012.01601.x

PHYLOGENETIC COMPARISON OF NEURON AND GLIA DENSITIES IN THE PRIMARY VISUAL CORTEX AND HIPPOCAMPUS OF CARNIVORES AND PRIMATES

Eric Lewitus,[1,2] Patrick R. Hof,[3] and Chet C. Sherwood[4]

[1]*Department of Anthropology, University College London, London WC1H 0BW, United Kingdom*

[2]*E-mail: lewitus@mpi-cbg.de*

[3]*Fishberg Department of Neuroscience and Friedman Brain Institute, Mount Sinai School of Medicine, Box 1065, One Gustave L. Levy Place, New York 10029*

[4]*Department of Anthropology, The George Washington University, 2110 G Street NW, Washington, DC 20052*

Received July 19, 2011
Accepted January 31, 2012

A major focus of comparative neuroanatomy has been on whether the mammalian brain evolves in a concerted or a mosaic fashion. Workers have examined variation in the volume of different brain regions across taxa to test the degree to which selection is constrained by the timing of events in neural development. Whether a conserved neurogenetic program in the mammalian brain constrains the distribution of different cell types, however, has not yet been investigated. Here we tested for evidence of evolutionary constraints on the densities of different cell types in the primary visual cortex (V1) and the hippocampus in 37 primate and 21 carnivore species. Cellular densities in V1 and the hippocampus scale isometrically with respect to one another in carnivores, as predicted by the concerted evolution hypothesis. In primates, however, cellular distributions in the hippocampus and primary visual cortex show no correlations, which supports the hypothesis of mosaic brain evolution. We therefore provide evidence for the presence of constraints controlling the adult densities of different cell types in disparate regions of the mammalian brain, but also for specializations along the primate lineage. We propose that adaptations to modularity at the cellular level may carry a deep phylogenetic signal.

KEY WORDS: **Allometry, carnivores, cerebral cortex, development, primates.**

The mammalian brain is composed of structurally distinct cell groups, which are configured into topographical maps underlying sensorimotor and cognitive functions (Kaas 1982; Passingham et al. 2002; Krubitzer 2009). While it is clear that some species display remarkable behavioral specializations, and that certain brain areas are devoted to mediating quite specific behaviors, the degree to which one region can evolve independently of functionally unrelated regions is poorly understood. It has been suggested that the size of different brain regions evolves in concert due to constraints of neural developmental timing (Finlay and Darlington 1995). In contrast, it has been proposed that developmental constraints are not sufficient to overpower the ability of regions to evolve independently (Barton and Harvey 2000; de Winter and Oxnard 2001).

Comparative studies of connectivity and circuitry in the mammalian brain confirm many of the predictions of the concerted evolution hypothesis. Structural components in the transcerebellar loops, for example, have been observed to covary in size across species (Voogd 2003). Similarly, reduction in the amount of retinal afferents has been shown to cause corresponding reductions in the lateral geniculate nucleus and visual cortex (e.g., Rakic et al. 1991; Cooper et al. 1993; Dehay et al. 1996).

EVOLUTION
INTERNATIONAL JOURNAL OF ORGANIC EVOLUTION

Table 1. List of species by taxonomic classification[1].

Taxonomic group	Subgroup	Species	Taxonomic group	Subgroup	Species
Primates	*Strepsirrhini*	*Galago senegalensis*	*Carnivora*	*Caniformia*	*Mustela nigripes*
		Nycticebus coucang			*Neovison neovison*
		Lemur catta			*Mephitis mephitis*
		Eulemur mongoz			*Taxidea taxus*
		Microcebus murinus			*Procyon cancrivorus*
		Cheirogaleus medius			*Procyon lotor*
	Tarsiidae	*Tarsius bancanus*			*Nasua nasua*
		Tarsius syrichta			*Bassaricyon gabbii*
	Platyrrhini	*Callithrix geoffroyi*			*Potos flavus*
		Leontopithecus rosalia			*Ailurus fulgens*
		Saguinus oedipus			*Zalophus californianus*
		Cebus capucinus			*Callorhinus ursinus*
		Saimiri sciureus			*Phoca vitulina*
		Aotus trivirgatus			*Ursus maritimus*
	Pitheciidae	*Callicebus moloch*			*Canis lupus familiaris*
		Pithecia pithecia			*Canis latrans*
	Cercopithecinae	*Alouatta caraya*			*Vulpes vulpes*
		Alouatta palliata		*Feliformia*	*Panthera pardus*
		Ateles ater			*Felis catus*
		Macaca fascicularis (2)			*Puma concolor*
		Macaca mulatta (2)			*Crocuta crocuta*
		Macaca maura (5)			*Cynictis penicillata*
		Cercocebus torquatus			
		Mandrillus sphinx			
		Papio anubis (2)			
		Cercopithecus mitis			
		Cercopithecus nictitans			
		Erythrocebus patas (2)			
		Colobus angolensis			
		Trachypithecus francoisi			
	Hominoidea	*Pongo pygmaeus* (2)			
		Pan paniscus			
		Pan troglodytes (5)			
		Homo sapiens (6)			
		Gorilla gorilla (2)			
		Hylobates muelleri			
		Symphalangus syndactylus			

[1]The number of individuals sampled for each species is listed. Where no number is listed, only one individual was sampled.

Epigenetic population matching, wherein competition for some trophic factor produced by a target determines the number of projection neurons that survive the period of programmed cell death (Katz and Lasek 1978; Linden 1994; Yeo and Gautier 2004), may, in part, explain these phenomena. However, patterns predicted by epigenetic population matching are not observed universally—different species tend to elaborate pathways from a common source differently (Northcutt and Wulliman 1988)—and, without developmental data, it is impossible to say that the population matching is epigenetically controlled (see Bunker and Nishi 2002). It may be that epigenetic cascades operate successfully in linear circuits, but not in reticulate circuits, which is why an examination of the available evidence suggests that the structure of region sizes in the mammalian brain is neither completely constrained by developmental timing nor completely free to evolve independently.

Volumetric size, however, is a poor estimate of the cellular composition of brain tissue (Azevedo et al. 2009). Increasing evidence for phyletic variation in the cellular organization of homologous regions of mammalian brains (e.g., Preuss and Coleman 2002; Hammock and Young 2005; Hutsler et al. 2005; Sherwood and Hof 2007) has demonstrated that interspecific variation in

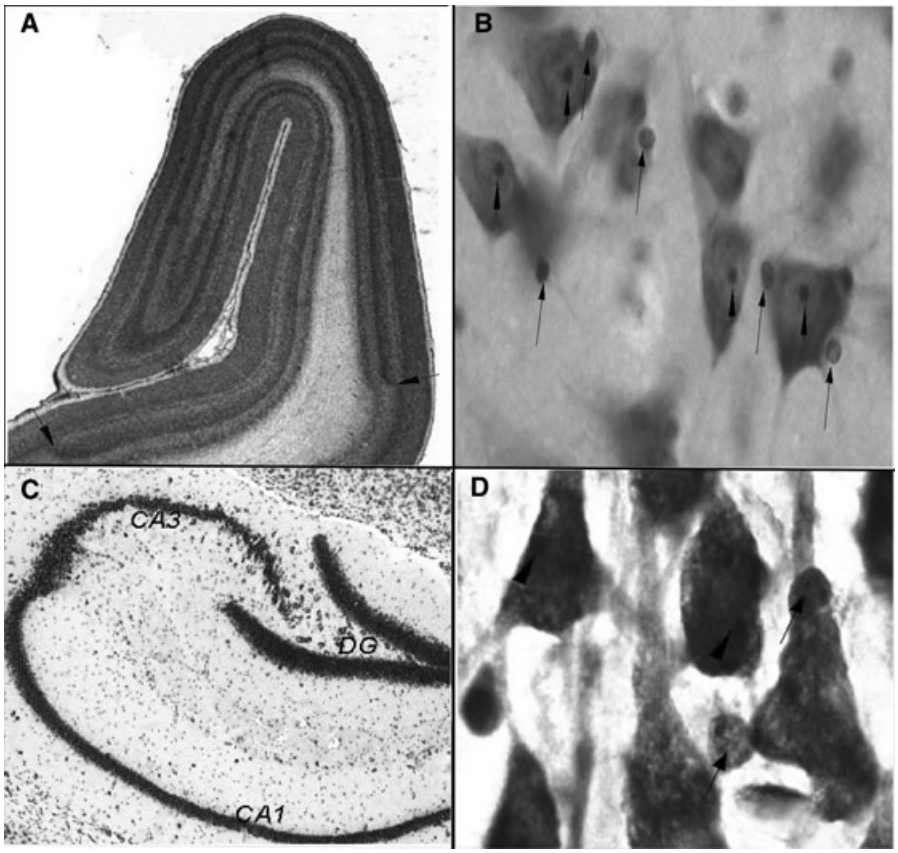

Figure 1. **Glia and neuron densities were counted in the primary visual cortex (A, B) and hippocampal subfields (C, D) using design-based stereology. (A) The mammalian V1 was demarcated (arrows) on the basis of its topological location and distinct appearance in materials stained for Nissl substance (Allman and McGuinness 1988; Hof and Morrison 1995; DeFelipe et al. 1999; Rosa and Krubitzer 1999; Rosa et al. 2005). The region of V1 sampled was restricted to layers II–VI due to tissue preservation in layer I. (C) Pyramidal cell regions of the hippocampus proper (*cornu ammonis*, CA) were demarcated at one end (CA3) by an abrupt change in the organization of neuronal cell bodies in the hilus (Rosene and Van Hoesen 1977; Amaral and Insausti 1990; Keuker et al. 2003) and at the other end (CA1) by the point at which the superficial cells of the hippocampus proper ceased to be contiguous (West et al. 1991; Keuker et al. 2003). Neurons in V1 (B) and the hippocampus (D) were distinguished from non-neuronal cells by the presence of dark, coarsely stained Nissl substance in the cytoplasm, a large nucleus, a distinct nucleolus, ovoid shape, and lightly stained proximal segments of dendritic processes. Glia were expected to lack a conspicuous nucleolus and contain less endoplasmic reticulum than neurons. Photo: A, *Callicebus moloch*; B, *Homo sapiens*; C, *Sorex araneus*; D, *Saguinus oedipus*.**

factors underlying brain size variation (e.g., cellular density, degree of dendritic arborization, and cell soma size) may also reflect evolutionary adaptations within lineages in conjunction with morphological or volumetric changes. Comparing cellular properties in disparate brain regions across taxa provides a new perspective to explore the extent to which developmental constraints act on the evolving mammalian brain.

Although the number of neurons in the cortex is approximately determined by the number of progenitor cells (Fish et al. 2008; Noctor et al. 2008), the duration of cell-division cycles (Lange et al. 2009), and the number of cell cycles during neurogenesis (Kornack and Rakic 1998), glia are generated only after neuronal migration terminates (Voigt 1989). The most abundant type of glial cells are astrocytes, which are distributed homogeneously in the cortical gray matter (Bushong et al. 2003; Nedergaard et al. 2003) and support neurons and the neuronal environment by producing trophic agents (Hatten et al. 1986; Müller et al. 1993; Araque et al. 1999; Barres and Smith 2001; Hidalgo et al. 2001; Allen and Barres 2005). Oligodendrocytes, glial cells that synthesize myelin, a lipid-rich membrane that ensheaths axons and increases the conduction velocity of electrical impulses, begin their differentiation after neurons have been surrounded by astrocytes and formed functional synapses (Baumann and Pham-Dinh 2001). The implication that astrocytes may regulate the generation of new neurons (Song et al. 2002; Horner and Palmer 2003; Nedergaard et al. 2003), influence the development and synaptogenesis of those neurons (Pfrieger and Barres 1997; Kang et al. 1998; Haydon 2001; Ullian et al.

Table 2. Stereologic estimates of cellular densities (cells per mm^3) in (A) nonprimate mammals and (B) primates.

	Primary visual cortex			Hippocampus		
Species	Glia–neuron ratio	Neuronal density	Glial cell density	Glia–neuron ratio	Neuronal density	Glial cell density
(A)						
Mustela nigripes	0.78	275,423	213,796	0.63	213,796	135,060
Neovison neovison	0.54	229,087	120,226	0.50	269,153	134,559
Mephitis mephitis	0.22	169,824	38,019	0.17	263,027	43,758
Taxidea taxus	1.07	77,625	83,176	0.52	194,984	102,329
Procyon cancrivorus	0.66	144,544	93,325	0.42	186,209	79,004
Procyon lotor	0.78	104,713	83,176	1.35	79,308	107,152
Nasua nasua	1.17	109,648	125,893	0.59	95,333	56,234
Bassaricyon gabbii	1.05	123,027	128,825	0.63	208,930	131,826
Potos flavus	0.76	186,209	141,254	0.91	147,911	134,896
Ailurus fulgens	1.07	154,882	165,959	1.12	95,499	106,989
Zalophus californianus	1.86	30,903	57,544	0.93	75,858	70,795
Callorhinus ursinus	1.7	63,096	104,713	1.82	60,256	109,648
Ursus maritimus	2.19	44,668	95,499	3.24	34,674	112,202
Canis lupus familiaris	0.76	204,174	158,489	0.35	288,403	102,304
Canis latrans	0.34	72,444	25,119	0.46	74,131	33,884
Vulpes vulpes	0.95	81,283	77,625	0.58	138,038	79,433
Panthera pardus	0.68	75,858	51,286	0.85	51,286	43,652
Felis catus	0.2	114,815	22,909	0.22	79,433	17,783
Puma concolor	1.07	69,183	74,131	0.95	87,096	83,176
Crocuta crocuta	1.26	63,096	79,433	0.98	64,565	63,096
Cynictis penicillata	0.87	141,254	123,027	0.68	115,025	78,101
(B)						
Callithrix geoffroyi	0.29	338,844	97,724	0.76	85,114	64,565
Leontopithecus rosalia	0.24	301,995	72,444	0.93	56,234	52,481
Saguinus oedipus	0.3	328,541	102,329	0.68	114,815	77,625
Cebus capucinus	0.17	245,471	41,687	0.66	114,900	75,858
Saimiri sciureus	0.25	478,630	117,490	0.65	113,200	74,131
Aotus trivirgatus	0.12	410,950	59,930	0.40	100,009	39,811
Callicebus moloch	0.27	467,735	125,893	0.71	102,329	72,444
Pithecia pithecia	0.58	169,824	97,724	0.38	45,162	17,378
Alouatta caraya	0.22	194,984	42,658	3.24	36,308	117,490
Alouatta palliata	0.28	176,349	49,168	0.81	81,283	66,069
Ateles ater	0.3	218,776	67,608	0.69	116,505	79,006
Macaca fascicularis	0.14	331,131	47,863	1.78	134,896	234,423
Macaca mulatta	0.27	422,149	113,783	1.58	67,608	107,152
Macaca maura	0.18	361,470	64,343	–	–	–
Cercocebus torquatus	0.39	426,580	165,959	1.02	60,256	61,660
Mandrillus sphinx	0.52	263,027	138,038	0.74	87,099	64,569
Papio anubis	0.51	275,423	141,254	0.47	194,984	89,125
Cercopithecus mitis	0.16	245,471	39,811	0.78	89,125	69,202
Cercopithecus nictitans	0.26	302,604	78,168	0.74	97,146	71,950
Erythrocebus patas	0.37	416,869	154,882	1.36	78,740	107,345
Colobus angolensis	0.23	223,872	51,286	1.48	75,858	109,648
Trachypithecus francoisi	0.33	446,684	147,911	0.72	112,202	79,433

Continued.

Table 2. Continued.

Species	Primary visual cortex			Hippocampus		
	Glia–neuron ratio	Neuronal density	Glial cell density	Glia–neuron ratio	Neuronal density	Glial cell density
(B)						
Pongo pygmaeus	0.96	151,356	144,544	–	–	–
Pan paniscus	0.62	218,776	134,896	3.09	44,668	138,038
Pan troglodytes	0.59	208,930	123,027	0.66	80,261	53,703
Homo sapiens	0.72	234,423	169,824	1.35	32,359	43,652
Gorilla gorilla	0.95	144,544	138,038	–	–	–
Hylobates muelleri	0.41	229,087	93,325	1.66	57,544	93,325
Symphalangus syndactylus	0.42	239,883	101,103	1.66	74,131	123,027
Tarsius bancanus	0.26	234,510	60,256	0.48	204,174	97,724
Tarsius syrichta	0.25	200,103	50,425	0.47	331,131	154,882
Lemur catta	0.85	70,795	60,256	0.79	87,096	69,183
Eulemur mongoz	0.59	234,423	138,038	0.61	117,490	71,328
Microcebus murinus	0.59	190,546	112,202	1.95	111,302	218,776
Cheirogaleus medius	0.59	186,209	109,648	2.00	107,152	213,796
Galago senegalensis	0.45	338,844	151,356	0.63	245,471	151,356
Nycticebus coucang	0.49	109,648	53,703	0.26	158,489	41,687

2001), monitor neurometabolic interactions at the synaptic cleft (Laming et al. 2000; Hertz et al. 2001), and generally be required for dense synaptic networks to achieve advanced degrees of local modulation and control, as well as the need for oligodendrocytes to bypass axonal size constraints in increasingly large brains (Wen and Chklovskii 2005), suggests that there might be an evolutionary role for a relative increase in glial cells.

Our aim was to test whether the density of neurons and glial cells covaries across different regions of the brain in carnivores and primates. The regions examined here—the primary visual cortex and subfields of the hippocampal formation—are not directly interconnected with one another and therefore may be free to evolve independently. Furthermore, these regions are well documented and can be reliably delineated in carnivores and primates. From evidence that the mammalian brain is loosely modularized (see Krubitzer 2007), such that one region is rarely isolated for specialization at the expense of others, but that the design of modularization itself can be selected, it is likely that the degree to which certain brain regions must evolve in concert and can evolve independently will carry a phylogenetic signal. In the current study, we compared neuronal and glial cell densities in the primary visual cortex (V1) and subfields of the hippocampus proper (CA1–3) in 37 primate species and 21 carnivore species. Our results provide evidence for concerted evolution of neuronal and glial cell densities in disparate regions of the carnivore brain, but also for specialization in the proportions of these different cell types along the primate lineage.

Materials And Methods

SPECIMENS

Samples of the left hemisphere of nonpathological postmortem brains representing 37 primate species and 21 carnivore species were used (Table 1). Eleven other eutherian species were also sampled (Table S1). All samples were from adult brains, except for *Trachypithecus francoisi* and *Pithecia pithecia*, which were from juveniles with brain sizes comparable to species-typical adult averages. Specimens from all collections were immersion fixed with either 10% formalin or 4% paraformaldehyde. Some brains were embedded in paraffin prior to sectioning. Brain sections were Nissl stained in the context of this research or unrelated experiments. The original research reported herein was performed under guidelines established by the Animals Scientific Procedures Act (ASPA). For the specimens sampled in the context of other investigations, it was impossible to control for artifacts related to discrepancies in fixation length and postmortem delay. The recorded brain weights in our sample, nonetheless, do not show significant deviations from species-typical average fresh weights. Comparable error in density estimates from tissue shrinkage and histological processing artifacts along both axes should be expected to affect the elevation of regressions, but not scaling exponents or residuals (see Sherwood et al. 2006). Because of concerns about the possible effect of unknown degrees of shrinkage artifact on variables, analyses were confined to only those that involved regressing density variables collected from the same specimens on themselves, containing equivalent effects of histological

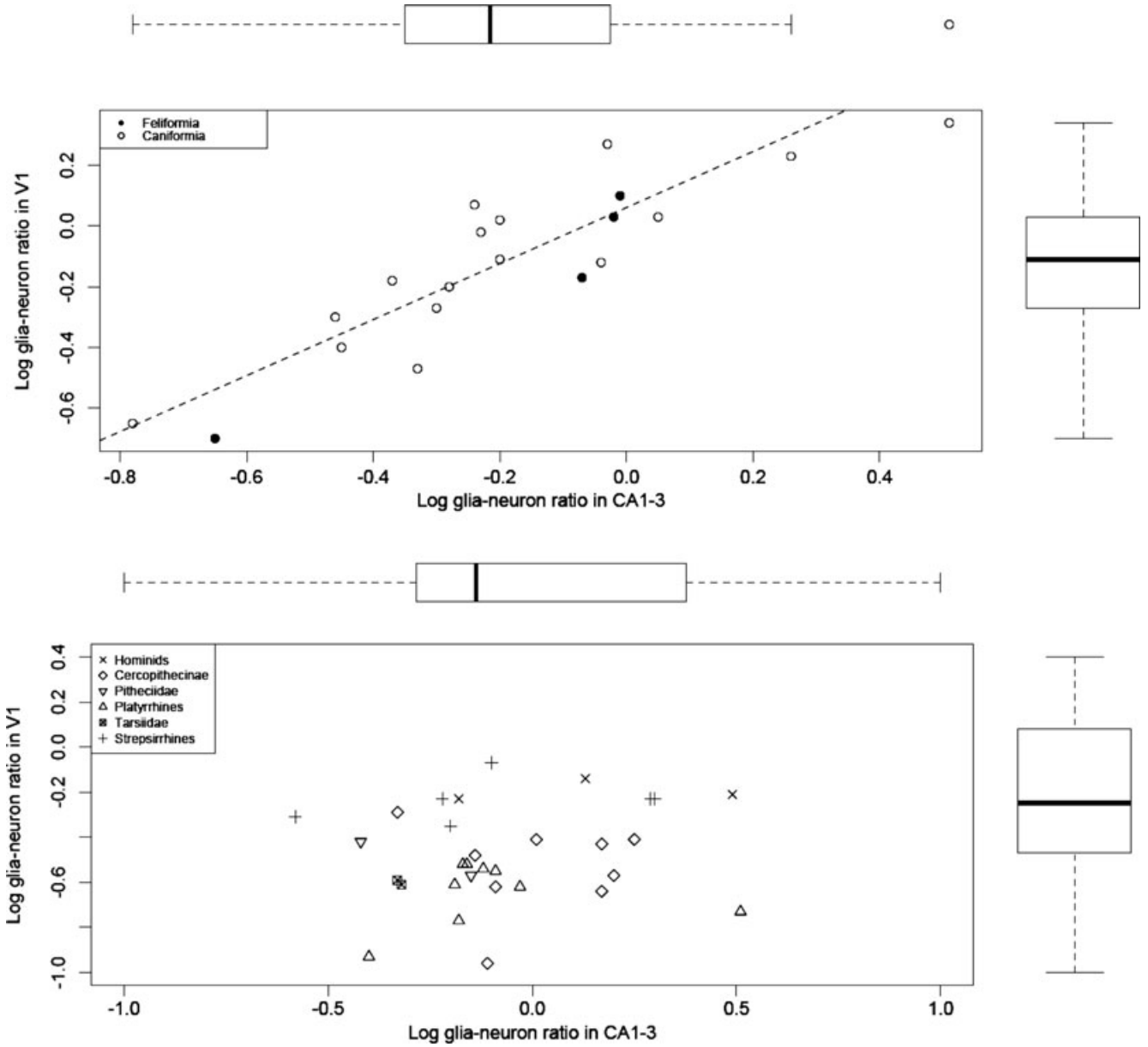

Figure 2. **Log-log regression plots of glia–neuron ratio in V1 and CA1–3 in carnivores (top) and primates (bottom). A significant scaling relationship, represented by the dotted line ($y = 0.923x + 0.061$, $R^2 = 0.814$, $P < 0.001$), was found in carnivores only. The bar graphs show group means for glia–neuron ratio in V1 (right) and CA1–3 (top), which are significantly different in carnivores and primates ($\chi^2 = 7.02$, $P = 0.030$).**

artifact in both x and y axes of the data derived from that individual.

STEREOLOGIC METHODS

We estimated the density of neurons and both astrocytes and oligodendrocytes (herein referred to as glia) in the primary visual cortex (V1) and hippocampal subfields (CA1–3). Demarcation of the hippocampus is explained in Figures 1 and S1L, and the demarcation of V1 has been explained previously (Lewitus et al. 2012). Excitatory and inhibitory neurons were not differentiated. No quantitative data were obtained on cell morphology, as it would have been outside the scope of our hypothesis, however, ease of identification of different cell types was not observed to change systematically across taxa. Cell counting was performed under bright-field microscopy using StereoInvestigator software (MBF Bioscience, Williston, VT). The thickness of sections cut from the microtome ranged from 25 to 100 μm. Mounted section thickness was measured at the first and final counting site for each section using the microcator with a 63× objective and used to calculate volume estimates for cellular densities by dividing the total estimated cell population by the mounted section thickness. For each individual, a random starting section was selected. Serial

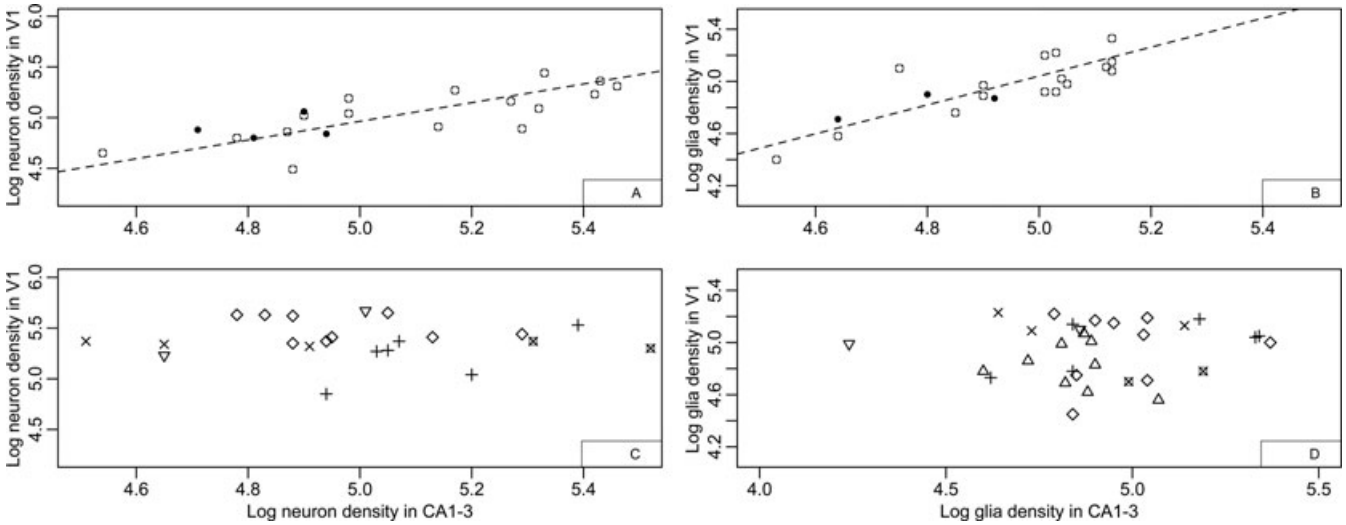

Figure 3. **Log-log regression plots for neuronal density and glial cell density in CA1–3 and V1 for carnivores (A, B) and primates (C, D). The dotted line represents SMA regressions fitted to carnivore species mean data ($R^2 > 0.75$, $P < 0.001$). All SMA exponents for species mean data and independent contrasts are presented in Table 3. See Figure 2 for legend.**

sections spaced at 300–400 μm were selected for analysis for each cell type. Boundaries of layers II–VI in V1 were outlined using a 10× objective, and a virtual 30 × 30 μm lattice of counting frames was randomly positioned on each slide to cover the sampled area with approximately 30 frames per section. Counting was performed under Koehler illumination using a 100× (NA 1.25, oil) objective—a 63× objective (NA 1.4, air) was used with one human individual and one chimpanzee individual, as the slides were too thick to allow for the working distance of higher power objectives. Because mounted section thickness varied, the disector thicknesses used also varied. A minimum 4-μm guard zone, defined as the space between the boundary of the tissue section and the part of the section used for counting, was set on either side of each section. Pilot tests were performed for each individual to determine the optimal size of the counting frame (approximately two cells per counting frame). The resulting coefficient of error (CE) was below 0.08 ± 0.01 for all analyses (Gundersen and Jensen 1987; Gundersen et al. 1999; Slomianka and West 2005). Cellular density was calculated as the sum of neurons counted with the disectors divided by the product of the sum of the disectors examined and the volume of the disector (Howard and Reed 1998). Volumetric estimates of the granular and molecular layer of the hippocampus and the granular layer of the cerebellum are presented as supplemental information (Table S2).

STATISTICAL ANALYSIS

Neuronal and glial cell densities of V1 and CA1–3 were plotted as functions of one another in carnivores and primates (Table 1). Scaling exponents were determined by standard major axis (SMA) line fitting based on log-transformed data. Independent contrasts were calculated using the PDAP:PDTREE module of Mesquite (Maddison and Maddison 2011) from a pruned mammalian phylogeny with the original branch lengths (Bininda-Emonds et al. 2007). Stepwise Akaike's information criterion (AIC) was used to determine the relative strengths of variables in predicting glia–neuron ratio in V1 and CA1–3 (Yamashita et al. 2007); Pearson product–moment correlations were used to determine linear dependence between cellular variables; and recursive trees and additional multiple regression metrics were used to determine the relative contributions of each variable to overall variation (Supporting information). Data within taxonomic groups were tested for homogeneity of variance with Bartlett's test and for normality with the Shapiro-Wilk's *W* test. Differences in distributions between taxonomic groups were tested using a two-sample Kolmogorov–Smirnov goodness-of-fit test. Kruskal–Wallis sum rank and multiple comparison tests were used to determine sample mean differences between groups. Statistical significance for all analyses was set at 0.05 (two tailed). All analyses were performed in *R* (version 2.13) with our own code and the package SMATR (Warton et al. 2006).

Results

Cellular variables in V1 and CA1–3 showed significantly different scaling patterns in primates and carnivores (Table 2A, B). In carnivores, glia–neuron ratio, neuronal density, and glial cell density in V1 were shown to scale isometrically with glia–neuron ratio, neuronal density, and glial cell density in CA1–3, respectively, for species mean data and independent contrasts (Figs. 2 and 3; Table 3). In primates, none of the variables in V1 scaled significantly with any of the variables in the hippocampus for species mean

Table 3. Slope estimates for scaling relationships based on cell densities (cells per mm^3).

Taxa	Dependent variable	Independent variable	Species mean data					Independent contrasts				
			SMA	R^2	Lower 95% CI	Upper 95% CI	P	SMA	R^2	Lower 95% CI	Upper 95% CI	P
Carnivores	Glia–neuron ratio in V1	Glia–neuron ratio in CA1–3	0.923	0.814	0.695	1.226	0.000	0.919	0.422	0.781	1.121	0.003
(n=21)	Neuron density in V1	Neuron density in CA1–3	0.922	0.751	0.671	1.268	0.000	0.997	0.292	0.808	1.246	0.025
	Glia density in V1	Glia density in CA1–3	1.11	0.862	0.871	1.410	0.000	1.183	0.685	0.994	1.467	0.000
	Glia–neuron ratio in V1	Brain mass (g)	0.419	0.554	0.284	0.619	0.009	0.300	0.483	0.308	0.699	0.031
	Glia–neuron ratio in CA1–3	Brain mass (g)	0.471	0.549	0.315	0.705	0.012	0.272	0.532	0.419	0.78	0.013
Primates	Glia–neuron ratio in V1	Glia–neuron ratio in CA1–3	0.923	0.019	0.695	1.226	0.565	−0.65	0.071	−0.528	−0.840	0.701
(n=37)	Neuron density in V1	Neuron density in CA1–3	0.922	0.015	0.671	1.268	0.605	0.630	0.154	0.499	0.805	0.361
	Glia density in V1	Glia density in CA1–3	1.108	0.042	0.871	1.409	0.386	0.728	0.080	0.537	0.906	0.670
	Glia–neuron ratio in V1	Brain mass (g)	0.341	0.256	0.244	0.477	0.138	−0.1	0.018	−0.510	0.362	0.469
	Glia–neuron ratio in CA1–3	Brain mass (g)	0.399	0.272	0.282	0.563	0.129	0.119	0.051	−0.277	0.470	0.208

data or independent contrasts (Table 3). Pearson product–moment correlations (PMCC) showed glia–neuron ratio ($R^2 = 0.814$, $P < 0.001$), neuronal density ($R^2 = 0.751$, $P < 0.001$), and glial cell density ($R^2 = 0.862$, $P < 0.001$) in V1 and CA1–3 to have strong linear dependences in carnivores. Furthermore, stepwise AIC multiple regressions showed glia–neuron ratio in CA1–3 to be the greatest predictor of glia–neuron ratio in V1 (t-value = 4.477, $P = 0.001$) and glial cell density in CA1–3 to be the greatest predictor of glial cell density in V1 in carnivores (t-value = 7.429, $P < 0.001$). Relative importance metrics and recursive tree models strongly supported these results (Figs. 4, S1A–S1K). In primates, PMCC showed no significant correlations between V1 and CA1–3 and no relative importance metric showed variables in V1 and CA1–3 to significantly predict or contribute to variance in one another.

We further tested glia–neuron ratio as a function of brain mass and showed significantly different correlations in carnivores and primates (Fig. 5; Table 3). In carnivores, glia–neuron ratio in both V1 and CA1–3 showed weak but significant ($R^2 < 0.590$, $P < 0.05$) correlations with brain mass. No significant correlations were found between brain mass and glia–neuron ratio in either V1 or CA1–3 in primates.

Group means of glia–neuron ratios in V1 showed homogeneity of variance ($K^2 = 0.403$, $P = 0.818$), as well as normality in primates ($W = 0.974$, $P = 0.612$) and carnivores ($W = 0.923$, $P = 0.098$). Group means of glia–neuron ratio in CA1–3 showed homogeneity of variance ($K^2 = 3.558$, $P = 0.169$), normality in primates ($W = 0.960$, $P = 0.201$) and carnivores ($W = 0.979$, $P = 0.925$), and normality of distribution between carnivores and primates ($D = 0.315$, $P = 0.165$).

Discussion

Most quantitative comparative studies of the mammalian brain have focused on the evolutionary relationships among different brain-region volumes (Jerison 1973; Gould 1975; Stephan et al. 1981; Finlay and Darlington 1995; Barton and Harvey 2000; Clark et al. 2001; Lefebvre et al. 2004; Yopak et al. 2010). However, no studies have yet considered the coordinated evolution of neuronal and glial cell distributions in regions of the neocortex and allocortex. As recent evidence has confirmed that volume and the total number of neurons in a given brain region show phylogenetically variable relationships to one another (Herculano-Houzel et al. 2006, 2007; Sarko et al. 2009; Herculano-Houzel 2010), investigating species diversity at the cellular level can help to identify evolutionary physiological constraints acting on the mammalian brain. Our data revealed significant relationships between neuron and glia in the primary visual cortex (V1) and hippocampal subfields (CA1–3) in carnivores that are not present in primates. Specifically, primates showed no significant scaling relationship

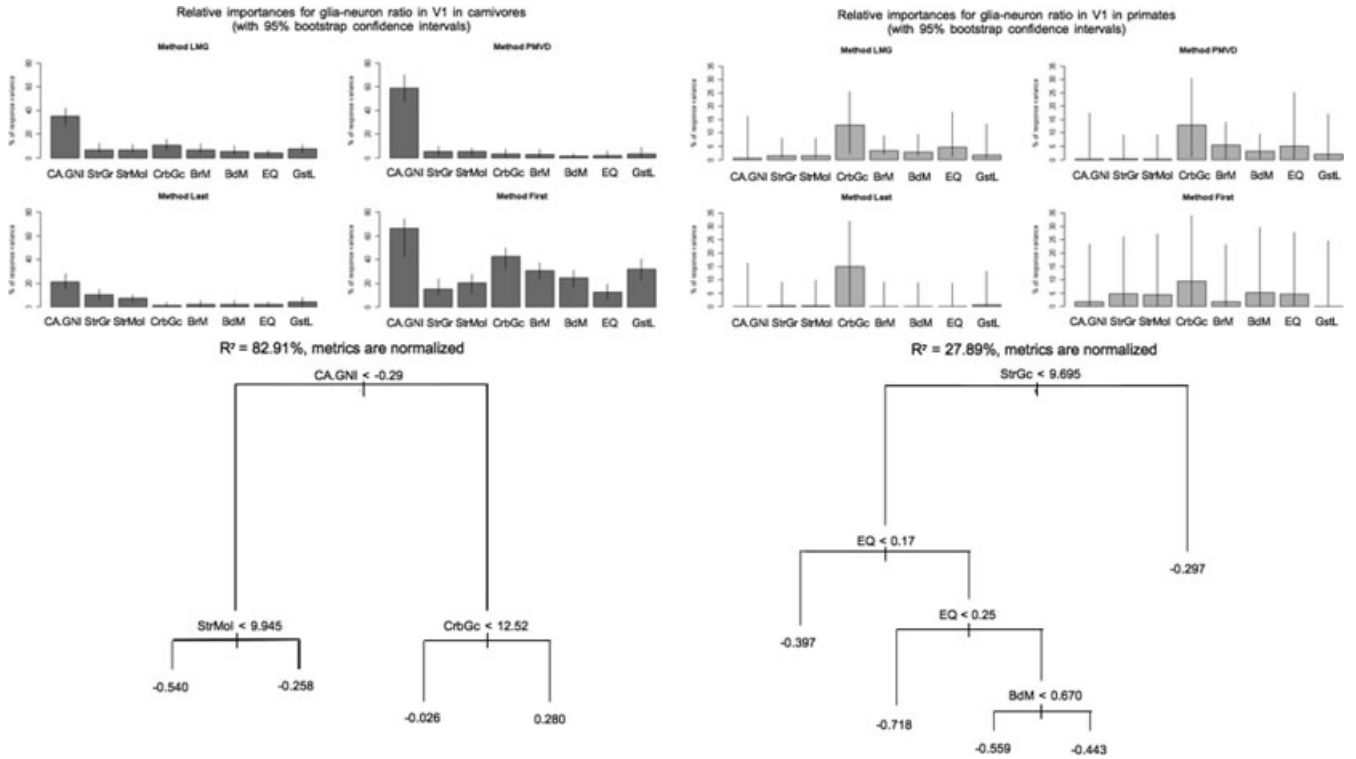

Figure 4. **Relative importance metrics (top) and recursive trees (bottom) for determining glia–neuron ratio in carnivores (left) and primates (right). In carnivores, the variables collectively explained 82.91% of the observed variance, with the contribution of glia–neuron ratio in CA1–3 shown to be significantly greater than that of any other variable for all metrics. The recursive tree shows glia–neuron ratio in CA1–3 to be the foremost and greatest contributor to variance in glia–neuron ratio in V1, *stratum moleculare* volume to be a significant contributor in species with a low glia–neuron ratio in CA1–3 (<0.51), and cerebellar granular layer volume to be a significant contributor in species with a large glia–neuron ratio in CA1–3 (>0.51). In primates, the variables collectively explained 28.79% of the observed variance. No variable is shown to contribute significantly more to variance than any other variable for all metrics. All variables in the recursive tree are log transformed and the branch lengths are representative of the deviance explained by each variable. Abbreviations: BdM = body mass (kg), BrM = brain mass (g), CA.GNI = glia–neuron ratio in CA1–3, CrbGc = volumetric estimate of the granule cell layer of the cerebellum (μm^3), EQ = encephalization quotient, GstLth = gestation length (days), StrGr = volumetric estimate of the *stratum granulosum* of the dentate gyrus (μm^3), StrMol = volumetric estimate of the *stratum moleculare* of the dentate gyrus (μm^3), V1.GNI = glia–neuron ratio in V1.**

between neurons and glia in V1 and CA1–3 and a remarkably different relationship between glia–neuron ratios in V1 and CA1–3 compared to all other eutherian species (Fig. 6; Table S3). We propose that the pattern observed in carnivores is indicative of constraints acting on evolutionary processes affecting mammalian brain development, and that the alteration of that pattern observed in primates represents a removal or relaxation of certain constraints. It is possible, for example, that evolutionary adaptations in the visual cortex in primates have influenced certain neurogenetic mechanisms, such as apoptosis (see Lietzau et al. 2009), and thus affected late-stage cell proliferation in other regions. Our data show that variation in the cellular organization of two diverse brain regions may be constrained along a mammalian lineage, but may also be relaxed or specialized along another lineage. As an induction of evolutionary change, the removal or relaxation of constraints may be a condition for adaptation.

In addition to interspecific differences in the number of cortical areas, with a proliferation of cortical areas generally following an increase in brain size (Krubitzer and Huffman 2000), interspecific differences in cortical cytoarchitecture have been shown to exist (Hof et al. 2000). Adaptations in cellular organization, which often represent isolated functional or behavioral variations and may be more easily interpreted than differences in cortical size across taxa (Sherwood et al. 2003, 2009; Hof et al. 2005; Raghanti et al. 2008; de Sousa et al. 2009, 2010), suggest that cellular reorganization may be one pathway to the independent specialization of brain regions. Our data agree with existing evidence showing the primate visual cortex to be, among mammals, especially derived (Preuss et al. 1999; Preuss and Coleman 2002) and that interspecific diversity in the cytoarchitecture of the visual cortex has arisen independently of brain size evolution (de Sousa et al. 2009, 2010). However, because the adult forms of cortical

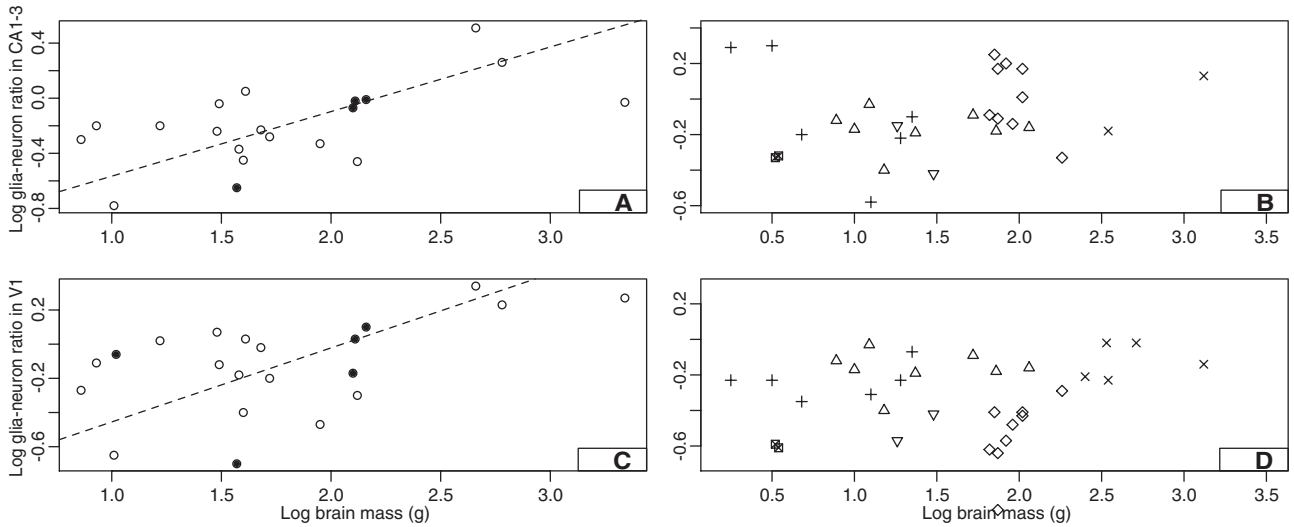

Figure 5. Carnivores show significant linear scaling relationships between brain mass and glia–neuron ratio in both CA1–3 (A; $y = 0.469x - 1.035$, $R^2 = 0.583$, $P = 0.007$) and V1 (C; $y = 0.434x - 0.899$, $R^2 = 0.531$, $P = 0.013$). Scaling relationships in primates for both CA1–3 (B) and V1 (D) do not reach significance for species mean data or independent contrasts (see Table 3). See Figure 2 for legend.

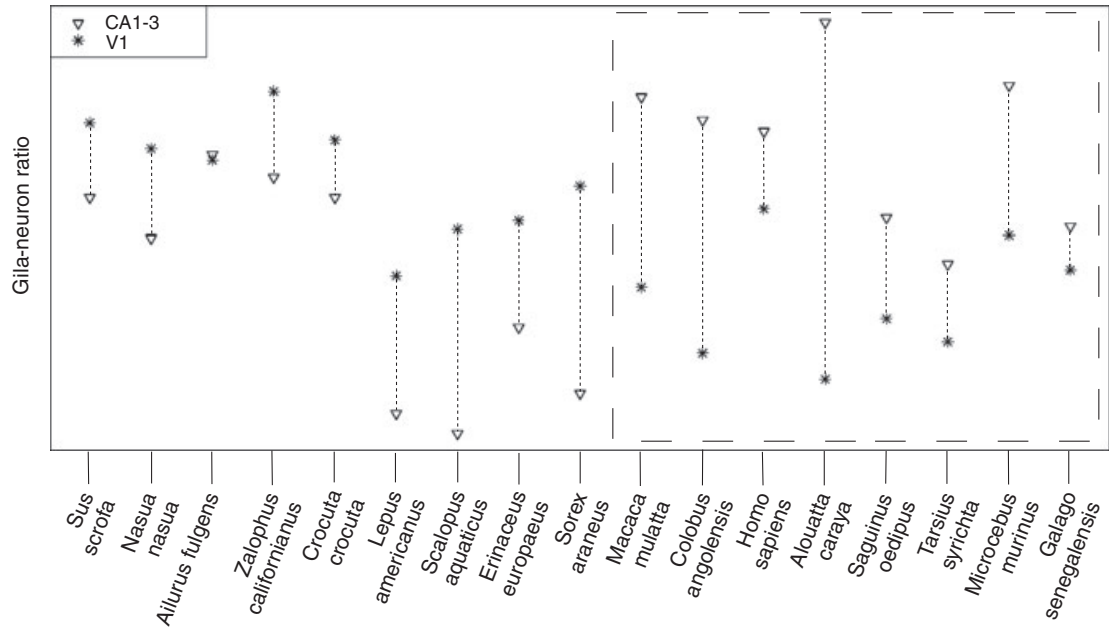

Figure 6. Glia–neuron ratios in V1 and CA1–3 for nonprimate and primate (dashed box) species show consistently higher values in V1 (mean = 1.05 ± 0.36) than in CA1–3 (mean = 0.78 ± 0.22) in nonprimates, but consistently lower values in V1 (mean = 0.41 ± 0.17) than in CA1–3 (mean = 1.07 ± 0.24) in primates. Mean values are significantly different in nonprimates and primates for both V1 ($T = 6.733$, $P < 0.001$) and CA1–3 ($T = -2.377$, $P = 0.021$) when all species are sampled (see Table S3).

areas are a result of developmental processes that associate diverse cortical regions, there is a fundamental difficulty in selecting one region without affecting all other developmentally associated regions. Although there is evidence for isolated cortical adaptation between, for example, nocturnal and diurnal rodents (Campi and Krubitzer 2010), concerted morphological evolution of cortical regions appears to be the prevailing trend (Finlay et al. 2001). But it is still unclear whether the same principle of concerted evolution applies to neurotransmitters, receptors, the expression of neuromodulators, and cell structure and organization. Is an increase

in glia to neurons in V1 likely to be accompanied a priori by a similar increase in the hippocampus? Is the principle of concerted evolution relevant at the cellular level? The observation that glia–neuron ratios in the neocortex and allocortex—or even brain size and body size—show tight statistical correlations within a particular mammalian order may simply mean that the only selection pressure acting to stabilize the relationship is a constraint on a developmental process. Additionally, the especially derived V1 in primates makes it difficult to conclude that all brain regions are more free to evolve independently in primates than in other mammals. In fact, homologous corticogenesis in carnivores and primates indicates that development of the cortex in mammals is influenced by similar constraints (Reillo et al. 2010; Kelava et al. 2012) and it is more likely, therefore, that selection on the proliferation of glia, which occurs subsequently to the proliferation of neurons, is responsible for the variation observed in this study. Comparative work on gliogenesis in mammals would be needed to test such a hypothesis.

We have provided evidence that diverse regions of the brain along a mammalian lineage are not de facto capable of evolving independently at the cellular level, with the implication that regions may only evolve independently following deep phylogenetic adaptations to conserved developmental processes.

ACKNOWLEDGMENTS

This work was supported in part by a grant from the J. S. McDonnell Foundation (22002078 to PRH and CCS; 220020293 to CCS), National Science Foundation (BCS-0827531 to CCS), National Institutes of Health (NS42867 to CCS), Brain Research Trust (EL), and University of London Central Research Fund (EL). EL would also like to thank Archibald Fobbs for help with the neuroanatomical collection at the NMHM (Washington, DC), C. Stimpson for assistance in preparation of many of the brains that were included in this study, and Evan Charles for discussion.

LITERATURE CITED

Allen, N. J., and B. A. Barres. 2005. Signaling between glia and neurons: focus on synaptic plasticity. Curr. Opin. Neurobiol. 15(5):542–548.

Allman, J.M., and E. McGuinness.1988. Primate visual cortex. Pp. 279–326 *in* H. Steklis, and J. Erwin, eds. *Comparative primate biology*. Neurosciences. John Wiley & Sons, Inc., New York.

Amaral, D. G., and R. Insausti. 1990. The human hippocampal formation. Pp. 711–755 *in* The human nervous system. Academic Press, San Diego.

Araque, A., R. P. Sanzgiri, V. Parpura, and P. G. Haydon. 1999. Astrocyte-induced modulation of synaptic transmission. Can. J. Physiol. Pharmacol. 77(9):699–706.

Azevedo, F. A. C., L. R. B. Carvalho, L. T. Grinberg, J. M. Farfel, R. E. L. Ferretti, R. E. P. Leite, W. J. Filho, R. Lent, and S. Herculano-Houzel. 2009. Equal numbers of neuronal and nonneuronal cells make the human brain an isometrically scaled-up primate brain. J. Comp. Neurol. 513:532–541.

Barres, B. A., and S. J. Smith. 2001. Neurobiology: cholesterol–making or breaking the synapse. Science 294(5545):1296–1297.

Barton, R., and P. H. Harvey. 2000. Mosaic evolution of brain structure in mammals. Nature 405:1055–1058.

Baumann, N., and D. Pham-Dinh. 2001. Biology of oligodendrocyte and myelin in the mammalian central nervous system. Physiol. Rev. 81(2):871–927.

Bininda-Emonds, O. R. P., M. Cardillo, K. E. Jones, R. D. E. MacPhee, R. M. D. Beck, R. Grenyer, S. A. Price, R. A. Vos, J. L. Gittleman, and A. Purvis. 2007. The delayed rise of present-day mammals. Nature 446:507–512.

Bunker, G. L., and R. Nishi. 2002. Developmental cell death in vivo: rescue of neurons independently of changes at target tissues. J. Comp. Neurol. 452(1):80–92.

Bushong, E. A., M. E. Martone, and M. H. Ellisman. 2003. Examination of the relationship between astrocyte morphology and laminar boundaries in the molecular layer of adult dentate gyrus. J. Comp. Neurol. 462(2):241–251.

Campi K. L., and L. Krubitzer. 2010. Comparative studies of diurnal and nocturnal rodents: differences in lifestyle result in alterations in cortical field size and number. J. Comp. Neurol. 518:4491–512.

Clark, D. A., P. P. Mitra, and S. S. H. Wang. 2001. Scalable architecture in mammalian brains. Nature 411(6834):189–193.

Cooper, H. M., M. Herbin, and E. Nevo. 1993. Visual system of a naturally microphthalamic mammal: the blind mole rat, *Spalax ehrenbergi*. J. Comp. Neurol. 328:313–350.

de Sousa, A. A., C. C. Sherwood, A. Schleicher, K. Amunts, C. E. MacLeod, P. R. Hof, and K. Zilles. 2009. Comparative cytoarchitectural analyses of striate and extrastriate areas in hominoids. Cereb. 20:966–981.

de Sousa, A. A., C. C. Sherwood, H. Mohlberg, K. Amunts, A. Schleicher, C. E. MacLeod, P. R. Hof, H. Frahm, and K. Zilles., A. A. 2010. Hominoid visual brain structure volumes and the position of the lunate sulcus. J. Hum. Evol. 58(4):281–292.

de Winter, W., and C. Oxnard 2001. Evolutionary radiations and convergences in the structural organizations of mammalian brains. Nature 409:710–714.

Defelipe, J., M. C. Gonzlez-Albo, M. R. Del Ro, and G. N. Elston. 1999. Distribution and patterns of connectivity of interneurons containing calbindin, calretinin, and parvalbumin in visual areas of the occipital and temporal lobes of the macaque monkey. J. Comp. Neurol. 412(3):515–526.

Dehay, C., P. Giroud, M. Berland, H. Killackey, and H. Kennedy.1996. Contribution of thalamic input to the specification of cytoarchitectonic cortical fields in the primate: effects of bilateral enucleation in the fetal monkey on the boundaries, dimensions, and gyrification of striate and extrastriate cortex. J. Comp. Neurol. 367:70–89.

Finlay, B. L., and R. B. Darlington. 1995. Linked regularities in the development and evolution of mammalian brains. Science 268:1578–1584.

Finlay, B. L., R. B. Darlington, and N. Nicastro. 2001. Developmental structure in brain evolution. Behav. Brain Sci. 24:263–278; discussion 278–308.

Fish, J. L., Dehay, C., Kennedy, H., and W. B. Huttner. 2008. Making bigger brains-the evolution of neural-progenitor-cell division. J. Cell Sci. 121:2783–2793.

Gould, S. 1975. Allometry in primates, with emphasis on scaling and the evolution of the brain. Contrib. Primatol. 5:244–292.

Gundersen, H. J. G., E. B. V. Jensen, K. Kieu, and J. Nielsen. 1999. The efficiency of systematic sampling in stereology—reconsidered. J. Microsc. 193(3):199–211.

Gundersen, H. J. G., and E. B. V. Jensen. 1987. The efficiency of systematic sampling in stereology and its prediction. J. Microsc. 147(3):229–263.

Hammock, E. A., and L. J. Young. 2005. Microsatellite instability generates diversity in brain and sociobehavioral traits. Science 308(5728):1630–1634.

Hatten, M. E., R. K. H. Liem, and C. A. Mason. 1986. Weaver mouse cerebellar granule neurons fail to migrate on wild-type astroglial processes in vitro. J. Neurosci. 6(9):2676–2683.

Haydon, P. G. 2001. Glia: listening and talking to the synapse. Nat. Rev. Neurosci. 2(3):185–193.

Herculano-Houzel, S. 2007. Encephalization, neuronal excess, and neuronal index in rodents. Anat. Rec. 290(10):1280–1287.

———. 2010. Coordinated scaling of cortical and cerebellar numbers of neurons. Front. Neuroanat. 4:12–20.

Herculano-Houzel, S., B. Mota, and R. Lent. 2006. Cellular scaling rules for rodent brains. Proc. Natl. Acad. Sci. USA 103(32):12138–12143.

Hertz, L., E. Hansson, and L. Rönnbäck. 2001. Signaling and gene expression in the neuron-glia unit during brain function and dysfunction: Holger Hydén in memoriam. Neurochem. Int. 39(3):227–252.

Hidalgo, A., E. F. V. Kinrade, and M. Georgiou. 2001. The drosophila neuregulin vein maintains glial survival during axon guidance in the CNS. Dev. Cell 1(5):679–690.

Hof, P. R., and J. H. Morrison. 1995. Neurofilament protein defines regional patterns of cortical organization in the macaque monkey visual system: a quantitative immunohistochemical analysis. J. Comp. Neurol. 352(2):161–186.

Hof, P. R., I. I. Glezer, E. A. Nimchinsky, and J. M. Erwin. 2000. Neurochemical and cellular specializations in the mammalian neocortex reflect phylogenetic relationships: evidence from primates, cetaceans, and artiodactyls. Brain Behav. Evol. 55(6):300–310.

Hof, P. R., R. Chanis, and L. Marino. 2005. Cortical complexity in cetacean brains. Anat. Rec. 287A(1):1142–1152.

Horner, P. J., and T. D. Palmer. 2003. New roles for astrocytes: the nightlife of an 'astrocyte'. La vida loca! Trends Neurosci. 26(11):597–603.

Hutsler, J. J., D. G. Lee, and K. K. Porter. 2005. Comparative analysis of cortical layering and supragranular layer enlargement in rodent carnivore and primate species. Brain Res. 1052(1):71–81.

Jerison, H. J. 1973. Evolution of the brain and intelligence. Academic Press, New York.

Jones, K. E., J. Bielby, M. Cardillo, S. A. Fritz, J. O'Dell, C. D. L. Orme, K. Safi, W. Sechrest, E. H. Boakes, C. Carbone, et al. 2009. PanTHERIA: a species-level database of life history, ecology, and geography of extant and recently extinct mammals. Ecology 90:2648–2648.

Kaas, J. H. 1982. The segregation of function in the nervous system: why do sensory systems have so many subdivisions? Contrib. Sens. Physiol. **7**:201–240.

Kang, J., L. Jiang, S. A. Goldman, and M. Nedergaard. 1998. Astrocyte-mediated potentiation of inhibitory synaptic transmission. Nat. Neurosci. 1(8):683–692.

Katz, M., and R. Lasek.1978. Evolution of the nervous system: role of ontogenetic buffer mechanism in the evolution of matching populations. Proc. Natl. Acad. Sci. USA 75:1349–1352.

Kelava, I., I. Reillo, A. Y. Murayama, A. T. Kalinka, D. Stenzel, P. Tomancak, F. Matsuzaki, C. Lebrand, E. Sasaki, J. C. Schwamborn, et al. 2012. Abundant occurrence of basal radial glia in the subventricular zone of embryonic neocortex of a lissencephalic primate, the common marmoset *Callithrix jacchus*. Cereb. Cortex 22: 469–481.

Keuker, J. I. H., C. D. P. Rochford, M. P. Witter, and E. Fuchs. 2003. A cytoarchitectonic study of the hippocampal formation of the tree shrew (*Tupaia belangeri*). J. Chem. Neuroanat. 26(1):1–15.

Kornack, D., and P. Rakic. 1998. Changes in cell-cycle kinetics during the development and evolution of primate neocortex. Proc. Natl. Acad. Sci. USA 95:1242–1246.

Krubitzer, L. 2007. The magnificent compromise: cortical field evolution in mammals. Neuron 56(2):201–208.

———. 2009. In search of a unifying theory of complex brain evolution. Ann. NY. Acad. Sci. 1156(1):44–67.

Krubitzer, L., and K. J. Huffman. 2000. Arealization of the neocortex in mammals: genetic and epigenetic contributions to the phenotype. Brain Behav. Evol. 55(6):322–335.

Laming, P. R., H. Kimelberg, S. Robinson, A. Salm, N. Hawrylak, C. Müller, B. Roots, and K. Ng. 2000. Neuronal-glial interactions and behaviour. Neurosci. Biobehav. Rev. 24(3):295–340.

Lange, C., W. B. Huttner, and F. Calegari. 2009. Cdk4/CyclinD1 overexpression in neural stem cells shortens G1, delays neurogenesis, and promotes the generation and expansion of basal progenitors. Cell Stem Cell. 5(3):320–331.

Lefebvre, L., S. M. Reader, and D. Sol. 2004. Brains, innovations and evolution in birds and primates. Brain Behav. Evol. 63(4):233–246.

Lewitus, E., C. C. Sherwood, and P. R. Hof. 2012. Cellular signatures in the primary visual cortex of phylogeny and placentation. Brain Struct. Funct. *In press*.

Lietzau, G., P. Kowiański, Z. Karwacki, J. Dziewiatkowski, M. Witkowska, J. Sidor-Kaczmarek, and J. Moryś. 2009. The molecular mechanisms of cell death in the course of transient ischemia are differentiated in evolutionary distinguished brain structures. Metab. Brain Dis. 24(3):507–523.

Linden, R. 1994. The survival of developing neurons: a review of afferent control. Neuroscience 58:671–682.

Maddison, W., and D. Maddison. 2011. Mesquite: a modular system for evolutionary analysis. Version 2.73. Available at: http://mesquiteproject.org/ (accessed June 15, 2011).

Müller, C. M., A. C. Akhavan, and M. Bette. 1993. Possible role of S-100 in glia—neuronal signalling involved in activity-dependent plasticity in the developing mammalian cortex. J. Chem. Neuroanat. 6(4):215–227.

Nedergaard, M., B. Ransom, and S. A. Goldman. 2003. New roles for astrocytes: redefining the functional architecture of the brain. Trends Neurosci. 26(10):523–530.

Noctor, S. C., V. Martínez-Cerdeño, and A. R. Kriegstein. 2008. Distinct behaviors of neural stem and progenitor cells underlie cortical neurogenesis. J. Comp. Neurol. 508(1):28–44.

Northcutt, R., and M. Wullimann. 1988. The visual system in teleost fishes: morphological patterns and trends. Pp. 515–552 *in* J. Atema, R. Fay, A. Popper, and W. Tavolga, eds. Sensory biology of aquatic animals. Springer, New York.

Passingham, R., Stephan, K., and R. Kötter. 2002. The anatomical basis of functional localization in the cortex. Nat. Rev. Neurosci. 3:606–616.

Pfrieger, F. W., and B. A. Barres. 1997. Synaptic efficacy enhanced by glial cells in vitro. Science 277(5332):1684–1687.

Preuss, T. M., and G. Q. Coleman. 2002. Human-specific organization of primary visual cortex: alternating compartments of dense Cat-301 and calbindin immunoreactivity in layer 4A. Cereb. Cortex 12(7):671–691.

Raghanti, M. A., C. D. Stimpson, J. L. Marcinkiewicz, J. M. Erwin, P. R. Hof, and C. C. Sherwood. 2008. Differences in cortical serotonergic innervation among humans, chimpanzees, and macaque monkeys: a comparative study. Cereb. Cortex 18(3):584–597.

Rakic, P., I. Suner, and R. W. Williams. 1991. A novel cytoarchitectonic area induced experimentally within the primate visual cortex. Proc. Natl. Acad. Sci. USA 88:2083–2087.

Reillo, I., C. de Juan Romero, M. A. Garcia-Cabezas, and V. Borrell. 2010. A role for intermediate radial glia in the tangential expansion of the mammalian cerebral cortex. Cereb. Cortex 21:1674–1694.

Rosa, M. G., and L. A. Krubitzer. 1999. The evolution of visual cortex: where is V2? Trends Neurosci. 22(6):242–248.

Rosa, M. G. P., S. M. Palmer, M. Gamberini, R. Tweedale, M. C. Piñon, and J. A. Bourne. 2005. Resolving the organization of the New World monkey third visual complex: the dorsal extrastriate cortex of the marmoset (*Callithrix jacchus*). J. Comp. Neurol. 483(2):164–191.

Rosene, D. L., and G. W. Van Hoesen. 1977. Hippocampal efferents reach widespread areas of cerebral cortex and amygdala in the rhesus monkey. Science 198(4314):315–317.

Rushton, W. 1951. A theory of the effects of fibre size in medullated nerve. J. Physiol. 115:101–122.

Sarko, D., K. C. Catania, D. B. Leitch, J. H. Kaas, and S. Herculano-Houzel. 2009. Cellular scaling rules of insectivore brains. Front. Neuroanat. 3:8.

Sherwood, C. C., and P. R. Hof. 2007. The evolution of neuron types and cortical histology in apes and humans. Pp. 355–378 *in* T. M. Preuss, and J. H. Kaas, eds. Evolution of nervous systems. Vol. 4. Academic Press, Oxford, U.K.

Sherwood, C. C., P. W. H. Lee, C. B. Rivara, R. L. Holloway, E. P. E. Gilissen, R. M. T. Simmons, A. Hakeem, J. M. Allman, J. M. Erwin, and P. R. Hof. 2003. Evolution of specialized pyramidal neurons in primate visual and motor cortex. Brain Behav. Evol. 61(1):28–44.

Sherwood, C. C., C. D. Stimpson, M. A. Raghanti, D. E. Wildman, M. Uddin, L. I. Grossman, M. Goodman, J. C. Redmond, C. J. Bonar, J. M. Erwin, et al. 2006. Evolution of increased glia-neuron rations in the human frontal cortex. Proc. Natl. Acad. Sci. USA 203:13606–13611.

———. 2009. Neocortical neuron types in Xenarthra and Afrotheria: implications for brain evolution in mammals. Brain Struct. Funct. 213:301–328.

Slomianka, L., and M. J. West. 2005. Estimators of the precision of stereological estimates: an example based on the CA1 pyramidal cell layer of rats. Neuroscience 136(3):757–767.

Song, H., C. F. Stevens, and F. H. Gage. 2002. Astroglia induce neurogenesis from adult neural stem cells. Nature 417(6884):39–44.

Stephan, H., H. Frahm, and G. Baron. 1981. New and revised data on volumes of brain structures in insectivores and primates. Folia Primatol. (Basel) 35(1):1–29.

Ullian, E. M., S. K. Sapperstein, K. S. Christopherson, and B. A. Barres. 2001. Control of synapse number by glia. Science 291(5504):657–661.

Voigt, T. 1989. Development of glial cells in the cerebral wall of ferrets: direct tracing of their transformation from radial glia into astrocytes. J. Comp. Neurol. 289:74–88.

Voogd, J. 2003. Cerebellum and precerebellar nuclei. Pp. 321–392 *in* G. Paxinos and J. May, eds. The human nervous system. Elsevier, San Diego.

Warton, D. I., I. J. Wright, D. S. Falster, and M. Westoby. 2006. Bivariate line-fitting methods for allometry. Biol. Rev. 81(2):259–291.

Wen, Q., and D. Chklovskii 2005. Segregation of the brain into gray and white matter: a design minimizing conduction delays. PLoS Comput. Biol. 1(7):e78.

West, M. J., L. Slomianka, and H. J. Gundersen. 1991. Unbiased stereological estimation of the total number of neurons in the subdivisions of the rat hippocampus using the optical fractionator. Anat. Rec. 231(4):482–497.

Yamashita, T., K. Yamashita, and R. Kamimura. 2007. A stepwise AIC method for variable selection in linear regression. Commun. Stat. A-Theor. 36(13):2395–2403.

Yeo, W., and J. Gautier 2004. Early neural cell death: dying to become neurons. Dev. Biol. 274(2):233–244.

Yopak, K. E., T. J. Lisney, R. B. Darlington, S. P. Collin, J. C. Montgomery, and B. L. Finlay. 2010. A conserved pattern of brain scaling from sharks to primates. Proc. Natl. Acad. Sci. USA 107(29):12946–12951.

Associate Editor: C. Farmer

Supporting Information

The following supporting information is available for this article:

Figure S1A. Recursive tree and relative importance metrics for determining glia-neuron ratio in CA1-3 in carnivores.
Figure S1B. Recursive tree and relative importance metrics for determining neuronal density in V1 in carnivores.
Figure S1C. Recursive tree and relative importance metrics for determining neuronal density in CA1-3 in carnivores.
Figure S1D. Recursive tree and relative importance metrics for determining glial cell density in V1 in carnivores.
Figure S1E. Recursive tree and relative importance metrics for determining glial cell density in CA1-3 in carnivores.
Figure S1F. Recursive tree and relative importance metrics for determining glia-neuron ratio in V1 in primates.
Figure S1G. Recursive tree and relative importance metrics for determining glia-neuron ratio in CA1-3 in primates.
Figure S1H. Recursive tree and relative importance metrics for determining neuronal density in V1 in primates.
Figure S1I. Recursive tree and relative importance metrics for determining neuronal density in CA1-3 in primates.
Figure S1J. Recursive tree and relative importance metrics for determining glial cell density in V1 in primates.
Figure S1K. Recursive tree and relative importance metrics for determining glial cell density in CA1-3 in primates.
Figure S1L. (Top) The hippocampal formation (HF) is located in the allocortex and consists of the *cornu ammonis* (CA) and the dentate gyrus (DG).
Figure S1M. The Nissl-stained cerebellum at 1× magnification (a, *Potos flavus*), 4× (b, *Mus musculus*), 10× (c, *Macaca mulatta*), and 40× (d, *M. musculus*) magnification.
Table S1. List of species by taxonomic classification*.
Table S2. Stereologic estimates of cellular densities (cells per mm^3) and volumetric estimates (mm^3) in nonprimate mammals.
Table S3. Stereologic estimates of cellular densities (cells per mm^3) and volumetric estimates (mm^3) in nonprimate mammals.

Supporting Information may be found in the online version of this article.

Please note: Wiley-Blackwell is not responsible for the content or functionality of any supporting information supplied by the authors. Any queries (other than missing material) should be directed to the corresponding author for the article.